Conductance fluctuations and field asymmetry of rectification in graphene

C. Ojeda-Aristizabal, M. Monteverde, R.Weil, M. Ferrier, S. Guéron, and H. Bouchiat

LPS, Univ. Paris-Sud, CNRS, UMR 8502, F-91405 Orsay Cedex, France

We investigate conductance fluctuations as a function of carrier density n and magnetic field in diffusive mesoscopic samples made from monolayer and bilayer graphene. We show that the fluctuations' correlation energy and field, which are functions of the diffusion coefficient, have fundamentally different variations with n, illustrating the contrast between massive and massless carriers. The field dependent fluctuations are nearly independent of n, but the n-dependent fluctuations are not universal and are largest at the charge neutrality point. We also measure the second order conductance fluctuations (mesoscopic rectification). Its field asymmetry, due to electron-electron interaction, decays with conductance, as predicted for diffusive systems.

PACS numbers:

Reproducible conductance fluctuations (CF) are one of the most striking signature of phase coherent transport [1]. The conductance of a mesoscopic sample results from interference between all wave packets traversing the sample. This interference pattern is sensitive to variations in disorder configuration, Fermi energy or magnetic flux, leading to reproducible CF as one of these parameters is changed. In diffusive or chaotic systems the CF amplitude has been shown to be universal [1–3] and ergodic, i.e. independent of the mechanism of phase randomization (magnetic field, Fermi energy, configuration of impurities for diffusive systems, sample shape for ballistic systems). The CF amplitude is of the order of e^2/h, with a coefficient which only depends on the symmetry class of the mesoscopic system. The typical correlation energies E_φ and fields B_φ of the fluctuations depend upon the typical time τ_{int} and area A_{int} over which interference occur: $E_\varphi = \hbar/\tau_{int}$ and $B_\varphi = \Phi_0/A_{int}$, with $\Phi_0 = h/e$ [2]. CF have been extensively investigated in metallic and semiconducting systems [1, 3]. The recently discovered graphene [4] provides a unique system in which the Fermi energy and diffusion constant can be tuned at will, over a broad carrier density range extending from hole to electron metallic conduction. Theoretical simulations of CF in graphene suggest a possible enhancement of the fluctuation amplitude with respect to standard mesoscopic samples, depending on the strength or nature of disorder (intervalley scattering) [5–7]. On the experimental side CF have been reported by several groups [8–13]. But to our knowledge the present work is the first complete investigation of their correlations and amplitudes as a function of Fermi energy and magnetic field, for both monolayer (ML) and bilayer (BL) graphene. The importance of the comparison lies in the fact that whereas ML and BL have similar resistivities and thus mean free paths (see Fig. 3), the (massless and massive) carriers have different velocities because of the different dispersion relations in these two materials. Thus the diffusion constants and therefore correlation energies and fields will have different carrier density dependences, providing a powerful test of the applicability of the theory of mesoscopic fluctuations in those systems. We find that the variations with carrier density n of the correlation field and energy are well related to those of the diffusion coefficient. We also find, in contrast with [10], that the amplitude of n-dependent fluctuations are largest near the charge neutrality point.

We also measure the second order conductance fluctuations [21] which, unlike linear conductance, are a probe of Coulomb interaction and screening, an important issue in graphene. Second order CF are inherent to systems lacking spatial inversion symmetry (because of random disorder in diffusive systems or geometry in ballistic systems). They stem from current-induced changes in the carrier density, which in turn, via Coulomb interaction, modify the electrostatic potential landscape, thereby inducing a current-dependent, or second order, change in the conductance of mesoscopic samples. Unlike the first order conductance which is even in field, the second order conductance has an odd part in field which was calculated for ballistic [16] and diffusive [17] systems. Whereas this mesoscopic rectification was experimentally investigated in ballistic mesoscopic systems (GaAs/GaAlAs quantum dots, Aharonov Bohm rings, carbon nanotubes [19, 20]), we provide in this letter the first measurement of second order CF in a diffusive system. We find, in qualitative agreement with theoretical predictions, that the odd in field rectification decreases with conductance.

Both ML and BL graphene samples (the nature of which was confirmed by Raman spectroscopy) were exfoliated and deposited onto doped silicon substrates with a 285 nm thick oxide. The electrodes were fabricated by electron beam lithography and sputter deposition of 40 nm thick palladium, providing low contact resistances (200 Ω for the ML and 20 Ω for the BL). The dimensions are $W = 2.7~\mu m$, $L = 0.8~\mu m$ and $W = 4.8~\mu m$, $L = 0.7~\mu m$ for the ML and BL, respectively (Fig. 3). The carrier density n is controlled for both systems by the voltage V_g applied to the doped silicon back gate, via $n = k_F^2/\pi = C(V_g - V_0)$, with C the gate capacitance per unit area, k_F the Fermi wave vector, and V_0 the gate voltage of the charge neutrality point. The transport pa-

rameters of both samples were determined via classical magnetoresistance measurement, described in [22]. We found that the transport mean free path l_{tr} of both ML and BL varies between 25 and 100 nm over the 60 V gate-voltage range probed. Thus l_{tr} is much smaller than the sample dimensions, so that both samples are in the diffusive regime. Two terminal resistance measurements were performed at 60 mK in a dilution refrigerator with resistive lines filtered at room temperature. The ac current amplitude I_0 was adjusted between 5 and 50 nA, depending on the sample resistance, to avoid heating while optimizing the signal to noise ratio. The first and second harmonics V_1 and V_2 of the ac voltage were measured with a low noise voltage preamplifier and a lock-in amplifier. The first and second order conductances were determined via $G_1 = I_0/V_1$ and $G_2 = 2V_2I_0/V_1^3$ [21]. The magnetic field was limited to less than 0.4 T, so that the contribution of Shubnikov de Haas oscillations is negligible. The CF of G_1 were measured as a function of B and V_g, for both the ML and BL (see Fig. 1). The V_g dependent fluctuations were analyzed in 3 V-wide windows, over which the density n can be considered practically constant. The fluctuations of G_1, even in B as expected in a two probe measurement, were characterized by their correlation functions and their amplitude δG_1, defined as the square root of their variance. The histogram of these fluctuations is Gaussian over the whole parameter range. The correlation gate voltage and field were determined in the following way. We calculated the Fourier power spectrum of the fluctuations as a function of k, the conjugate variable of B or V_g, for each set of field or gate voltage data corresponding to a given average carrier density. This spectrum is the Fourier transform of the correlation function of the fluctuations. Each dataset yielded exponential-like functions which correspond to a lorentzian correlation function in the direct space (Fig. 2a). The decay $exp(-kx_c)$ at low k yields the correlation gate voltage or field x_c for each dataset. The correlation energy E_c is related to the V_g correlation scale V_c by $E_c = V_c \hbar v_F \sqrt{\pi C/(4eV_g)}$ for the ML and $\hbar^2 \pi C V_c/(2em_{eff})$ for the BL, with $m_{eff} = 0.03m_e$ the (constant) low energy effective mass in the BL. These relations are incorrect near the charge neutrality point (CNP) because of density inhomogeneities, so that we deduced E_c from V_c via $k_F(V_g)$ determined in [22].

In Fig.2 we compare the variations of E_c and B_c to the predictions [2] $E_\varphi = \hbar D/L_{min}^2$ and $B_\varphi = \Phi_0/(L_{min}W_{min})$, where $L_{min} = min(L, L_T, L_\varphi)$ and $W_{min} = min(W, L_T, L_\varphi)$ correspond to the typical longitudinal and transverse length of interfering trajectories; $L_T = \sqrt{\hbar D/k_B T}$ and L_φ are respectively the thermal and the phase coherence length. We first determine the diffusion coefficient $D = \sigma/(e^2\nu(E_F)) = v_F l_{tr}/2$, where σ is the conductivity and $\nu(E_F)$ is the density of states, v_F is constant (10^6 m/s) for the ML and is $\hbar k_F/m_{eff}$
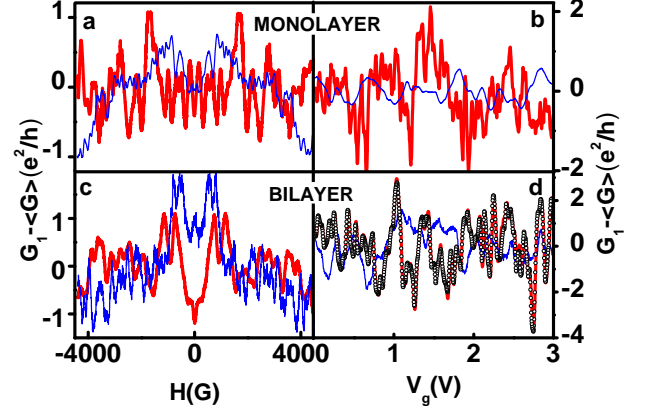

FIG. 1: CF as a function of magnetic field (left) and gate voltage (right). A linear fit was subtracted to remove the average conductance. Thick red (resp. thin blue) curves are measured around $V_g = V_0$, the charge neutrality point (CNP) (resp. at high carrier density, corresponding to $V_g - V_0 = 40.5$ V for the ML and $V_g - V_0 = 15$ V for the BL). The CNP is at $V_0 = 15.5$ V for the ML and $V_0 = -6$ V for the BL. It is clear (b,d) that the amplitude of V_g-dependent CF is larger at the CNP than at high density, both for the ML and the BL. Panel d also shows the reproducibility of the CF, via two nearly indistinguishable successive gate voltage sweeps (open dots and red line).

for the BL. Both l_{tr} and k_F were extracted in [22]. We find that at 60 mK L_T varies between 0.7 and 1.8 μm, so that $L < L_T < W$ for both samples over the entire density range investigated. Thus $W_{min} = L_T$ and $L_{min} = L$. Consequently E_c is expected to vary like the Thouless energy $E_{Th} = \hbar/\tau_D = \hbar D/L^2$, and B_c like $\Phi_0/(LL_T)$ [14]. As shown in Fig. 2, this is indeed what is found: the correlation energy deduced from the experimental data follows $E_c = 5 E_{Th}$, and the correlation field follows $B_c = 6 \Phi_0/(LL_T)$ for the ML and $B_c = 4 \Phi_0/(LL_T)$ for the BL. In particular, we find the expected linear dependence of E_c with D, which itself varies like V_g for the BL and $\sqrt{V_g}$ for the ML. This stems from the fact that in both samples the conductance varies linearly in $n \propto V_g$ within logarithmic corrections [22], and that $\nu(E_F)$ is independent of V_g for the BL and varies like $\sqrt{V_g}$ for the ML. Similarly $B_c \propto \Phi_0/LL_T$ is expected to vary like $D^{-1/2} \propto V_g^{-1/2}$ and $V_g^{-1/4}$, as observed respectively for the BL and ML. The numerical factors may be explained by the samples' aspect ratios, but more theory is needed to assess this point.

We now discuss the CF amplitude. As is visible in figures 1b and 1d, the V_g-dependent CF are greater near the CNP. This is quantified by the fluctuation amplitude δG_1 plotted as a function of V_g in Fig. 3. In contrast, the B-dependent fluctuations do not significantly depend on the density n. This non ergodicity of the fluctuations in
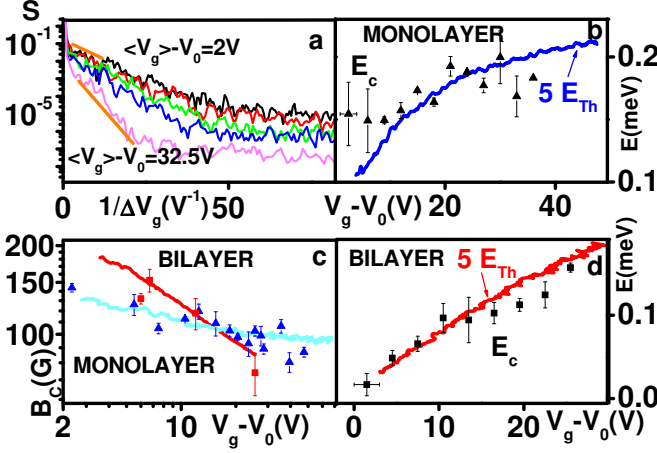
FIG. 2: Correlation energies and fields of CF. (a) Fourier power spectrum of CF at different V_g in a semi-log scale. V_c is extracted from the exponential fit at small ΔV_g^{-1}. (b) and (d): $E_c(V_g)$ for the ML and BL. Continuous lines are $5E_{Th}$, with D determined from previous magnetoresistance measurements (see text). (c): $B_c(V_g)$. Continuous lines are $B_\varphi = 6\Phi_0/(L_T L)$ for the ML and $4\Phi_0/(L_T L)$ for the BL, with D similarly determined. Vertical error bars represent uncertainty in fit parameters, and horizontal bars the 3 V range used to calculate correlation energies.

graphene may be a consequence of the spatial inhomogeneities of n close to the CNP. Indeed, in a good conductor (large g), changing the Fermi energy is equivalent to changing the disorder configuration, and induces CF of order e^2/h. In graphene on the other hand, it has been shown [23] that near the CNP the system breaks into conducting puddles of electrons and holes, and that transport takes place along an intricate percolating network of these n and p-type regions [6]. Thus, as pointed out in [5], the change in configuration induced by a change of V_g in this region may induce a much larger variation of conductance than a change in the disorder configuration in a good conductor. In contrast, the magnetic field does not affect the network but only the phases of the wave functions, which explains why the fluctuations with B are independent of gate voltage [5]. Note that these results are in contradiction with those of [10] who found a smaller CF amplitude close to the CNP. This discrepancy could be due to a different nature of disorder in the samples [5]. For the ML, we find the B-dependent CF amplitude to be 0.4 ± 0.1 e^2/h, independent of V_g. Theory [2] predicts $\delta G = 0.7\sqrt{W/L}$ e^2/h when the distance between electrodes L is smaller than L_T. This yields $\delta G = 1.2$ e^2/h for the ML, which is three times the value measured in this work (Fig. 3).

We now turn to second-order non-linear CF in monolayer graphene. As mentioned in the introduction, current through a mesoscopic sample induces charge accumulation around impurities and sample edges. This
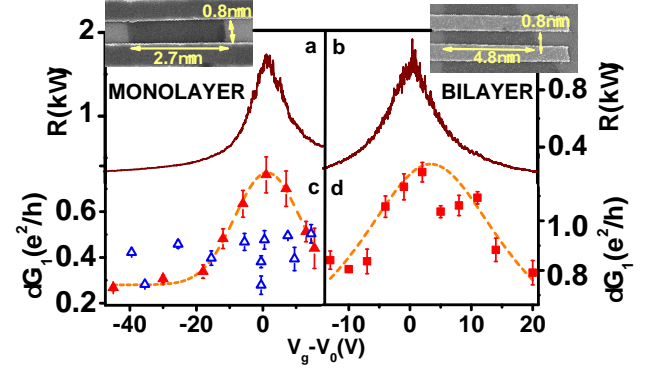

FIG. 3: Comparison between resistance and CF. The V_g-dependent fluctuations (filled symbols) are larger near the CNP for both the ML and BL (panels c and d). Error bars are the standard deviation of the difference of two different sweeps. Dashed lines are guides for the eyes. The V_g-dependent fluctuation amplitude changes with V_g in a qualitatively similar way as the resistance. The B-dependent CF amplitude (open triangles) doesn't change much with V_g.

bias induced change of electronic density $\delta n(r, V)$ modifies (via Coulomb interactions) the electrostatic potential landscape throughout the sample by $\delta U_{dis}(\gamma_{int}, V)$, where γ_{int} quantifies e-e interactions [15]. As a result, CF acquire a non linear bias dependent contribution : $G = G[U_{eq}] + \delta G[\delta U_{dis}(\gamma_{int}, V)]$, where U_{eq} is the potential in zero bias. $G_1 = G[U_{eq}(r)]$ is the linear conductance, and $G_2 = (\partial G[\delta U_{dis}, V, \gamma_{int}]/\partial V)_{V=0}$ is the second order conductance. In a magnetic field B, $\delta n(r, V)$ and $\delta U_{dis}(\gamma_{int}, V)$ contain a component which is even, as well as another which is odd in B, which can be viewed as a mesoscopic Hall voltage. Contrary to G_1 which is even in B, in the presence of interactions G_2 has a component which is odd in B, G_2^{AS}. The ratio between the even (symmetric) variance δG_2^S and the odd (antisymmetric) variance δG_2^{AS} of G_2 is predicted to be independent of conductance in ballistic systems, but in diffusive systems it should vary like $\frac{\delta G_2^{AS}}{\delta G_2^S} = \frac{\gamma_{int}}{g}$, with g the conductance in units of e^2/h [17, 18]. Figure 4 shows G_2^S and G_2^{AS} at two different carrier densities (close and far from the CNP), as well as the ratio of the odd to even amplitude $r = \frac{\delta G_2^{AS}}{\delta G_2^S}$. We find that r significantly decreases as carrier density increases, in contrast to ballistic GaAs/GaAlAs rings [20], where r was nearly independent of the dimensionless conductance g. To compare to the predictions for diffusive systems, $r = \gamma_{int}/g$, we plot in Fig. 4c $r(V_g)$, and find that $r \approx (7 \pm 1)/g$. According to [16], the interaction constant γ_{int} is related to the geometrical capacitance C and electro chemical capacitance $C_\mu = (1/(\nu e^2) + 1/C)^{-1}$ by $\gamma_{int} = C_\mu/C$. Thus $\gamma_{int} = 1/(1 + C/(\nu e^2))$ [16]. Perfect screening (in materials with large densities of states) corresponds to

conductance to find that its field asymmetry decreases with g, in agreement with theoretical predictions for diffusive systems. This indicates strongly screened electron-electron interactions in graphene.
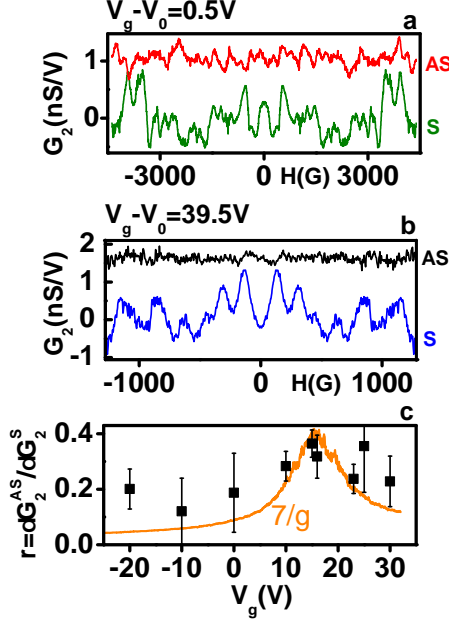
FIG. 4: Second order conductance fluctuations for the ML, near (a) and far (b) from the CNP. The antisymmetric part $G_2^{AS} = (G_2(H) - G_2(-H))/2$ is largest at the CNP. (c)The ratio $r = \delta G_2^{AS}/\delta G_2^S$ is compared to $7/g$. Error bars are deduced from the difference of $G_2(H)$ between two consecutive scans, which is mainly due to telegraphic noise in the sample.

$\gamma_{int} = 1$, and no screening to $\gamma_{int} = 0$. In graphene $\gamma_{int} \approx 1$ over the entire n range investigated, within less than 4/1000 : screening is strong, even close to the CNP where $\gamma_{int} = 0.996$. The factor 7, compared to 1 expected for $L = W$, may be due to the large aspect ratio W/L of the sample, which is known to increase δG_1 entering in the calculation of r [20], but there are no calculations for our geometry.

In conclusion we have shown that mesoscopic graphene samples exhibit conductance fluctuations which Fermi energy- and $B-$dependent correlation functions can be described by theoretical predictions for diffusive systems over a wide range of carrier concentration, for both monolayer and bilayer. The different behaviors of the correlation energy and fields are intimately related to the fundamentally different dispersion relations of both systems. A significant increase of the amplitude of the Fermi energy-dependent fluctuations is observed close to the neutrality point, whereas the B-dependent fluctuation amplitude is nearly constant over the entire carrier density range. This non-ergodicity of fluctuations may be attributed to the particular disorder due to electron and hole puddles in graphene near the Charge Neutrality Point. Finally, we have measured the second order non-linear conductance. We have exploited the tunability of graphene's

[1] See, e.g., *Mesoscopic Phenomena in Solids*, ed. B.L. Altshuler, P.A. Lee and R.A. Webb (Elsevier, Amsterdam, 1991); Y. Imry, *Introduction to Mesoscopic Physics* Oxford UP, New York, 1997, E. Akkermans and G. Montambaux, *Mesoscopic Physics with electrons and photons*, Cambridge University Press, (2007).
[2] B.L. Altshuler, JETP Lett.41 648 (1985); P. A. Lee, A. D. Stone, H. Fukuyama, Phys. Rev. B 35, 1039 (1987).
[3] S. Washburn and R. A. Webb, Adv. in Phys. 35, 375 (1986).
[4] K. S. Novoselov *et al.*, Nature 438, 197-200 (2005).
[5] A. Rycerz, J. Tworzydlo and C. W. J. Beenakker, Europhys. Lett. 79, 57003 (2007).
[6] V. V. Cheianov *et al.*, Phys. Rev. Lett. 99, 176801 (2007).
[7] M. Y. Kharitonov and K. B. Efetov, Phys. Rev. B 78, 033404 (2008).
[8] C Berger *et al.*, Science 3012, 1191 (2006).
[9] H.B. Heersche *et al.*, Nature 446, 56 (2007).
[10] N. E. Staley, C. P. Puls, and Y. Liu, Phys. Rev. B 77, 155429 (2008).
[11] K. Kechedzhi *et al.*, Phys. Rev. Lett. 102, 066801 (2009).
[12] M.B. Lundenberg and J.A. Folk, arxiv 0904.2212, to appear in Nature Physics (2009)
[13] J. Berezovsky and R. Westervelt, arxiv0907.0428(2009).
[14] We have assumed $L_\varphi > L_T$, which is always true when phase coherence is limited by electron-electron interactions. Note also that ref. [11] explores the different, high temperature regime where $E_\varphi = k_B T$.
[15] T. Christen and M. Büttiker, Eur. Phys. Lett. **35**, 523 (1996).
[16] D. Sanchez and M. Büttiker, Phys. Rev Lett. 93, 106802 (2004).
[17] B. Spivak and A. Zyuzin, Phys. Rev. Lett. 93, 226801 (2004).
[18] M. L. Polianski and M. Büttiker, Phys. Rev. Lett. **96**, 156804 (2006)
[19] J. Wei *et al.*, Phys. Rev. Lett. **95**, 256601 (2005),A. Löfgren *et al.*, Phys. Rev. Lett. **92**, 46803 (2004); D. M. Zumbühl *et al.*, Phys. Rev. Lett. **96**,206802 (2006); R. Leturcq *et al.*, Phys. Rev. Lett. **96**, 126801 (2006).
[20] L. Angers *et al.*, Phys. Rev. B 75, 115309 (2007).
[21] G_2 is defined as $I = G_1 V + G_2 V^2 + ...$

[22] M. Monteverde *et al.*, Phys. Rev. Lett. **104**, 126801 (2010).

[23] J. Martin *et al.*, Nat. Phys. 4, 144 (2008).